PAPER

Fully stretchable textile-based triboelectric nanogenerators with crepe-paper-induced surface microstructures

Da Eun Kim, [ID] Siho Shin, Gengjia Zhang, Daegil Choi and Jaehyo Jung*

Currently, major energy sources such as fossil fuels and nuclear fuels face various issues such as resource depletion, environmental pollution, and climate change. Therefore, there is increasing interest in technology that converts mechanical, heat, vibration, and solar energy discarded in nature and daily life into electrical energy. As various wearable devices have been released in recent years, wearable energy-harvesting technologies capable of self-power generation have garnered attention as next-generation technologies. Among these, triboelectric nanogenerators (TENGs), which efficiently convert mechanical energy into electrical energy, are being actively studied. Textile-based TENG (T-TENGs) are one of the most promising energy harvesters for realizing wearable devices and self-powered smart clothing. This device exhibited excellent wearability, biocompatibility, flexibility, and breathability, making it ideal for powering wearable electronic devices. Most existing T-TENGs generate energy only in the intentional vertical contact mode and exhibit poor durability against twisting or bending deformation with metals. In this study, we propose a sandwich-structured T-TENG (STENG) with stretchability and flexibility for use in wearable energy harvesting. The STENG is manufactured with a structure that can maintain elasticity and generate a maximum voltage of 361.4 V and current of 58.2 µA based on the contact between the upper and lower triboelectric charges. In addition, it exhibited a fast response time and excellent durability over 5000 cycles of repetitive pushing motions. Consequently, the STENG could operate up to 135 light-emitting diodes (with output) without an external power source, and as an energy harvester, it could successfully harvest energy for various operations. These findings provide textile-based power sources with practical applications in e-textiles and self-powered electronics.

Introduction

With the rapid development of the Internet of Things (IoT) technology, the demand for portable and wearable electronic products has increased. With the emergence of the wearable electronics market, studies on energy technologies that can supply power to portable/small electronic products have been conducted.[1–3] In particular, energy-harvesting technology that regenerates mechanical energy discarded in the surrounding environment (*e.g.*, body energy, vibration, heat, and electrons) into electrical energy is in the spotlight. Among these, studies on triboelectric nanogenerators (TENGs), which efficiently convert mechanical energy into electrical energy, are being actively conducted.[4,5]

TENG produce electrical outputs based on the combined effects of electrostatic induction and contact–frictional electrification.[6,7] In triboelectric electrification, materials are positively or negatively charged when they come into contact with or are separated by an external force. Based on the type of friction

material and electrode position, TENGs are divided into four operating modes: vertical contact–separation, lateral sliding, single-electrode, and free-standing. In the vertical contact–separation mode, the TENG comprises two different friction materials and generates an electrical output based on the contact and separation of the friction materials. In this mode, the TENG is attached to the soles of most shoes to generate electricity based on the movement of people in daily life (*e.g.*, walking or running) and can be easily manufactured at a low cost with a simple structure. The operation of the lateral sliding mode is similar to that of the vertical contact separation mode; however, this mode generates an electrical output based on the movement of parallel translation in a state where two different friction materials are not separated. This mode exhibits a better output performance because it has a larger contact area than the vertical contact mode. The single-electrode mode exhibited the simplest mechanism of action. It requires only one electrode and the friction material can move freely without being constrained. However, the single-electrode mode is suitable for portable and self-powered systems because of its lower output performance compared with other modes. Unlike other modes, the freestanding mode comprises two electrodes and a vertical

AI Healthcare Research Center, Department of IT Fusion Technology, Chosun University, Chosundaegil 146 (Seo-seok-dong), Dong-gu, Gwangju, 61452, South Korea. E-mail: Jh.jung@chosun.ac.kr

or horizontal friction material. In this mode, a high electrical output can be obtained because there is no need to maintain contact.[8] In this mode, the friction material moves freely. TENG technology possesses distinct advantages, such as a variety of material choices, productivity, wearability, wide usability, and low manufacturing cost. Recently, several studies have been conducted on textile-based TENGs (T-TENGs) with high performance and wearability, which can efficiently harvest energy based on human body motions.

Textiles possess various advantages such as flexibility, elasticity, durability, permeability, light weight, and biocompatibility; therefore, they are used as friction materials for TENGs.[9–11] Moreover, textiles can efficiently harvest energy through friction with materials possessing different electron affinities; the greater the relative difference in the electron affinity, the higher the power generated. T-TENGs can harvest large amounts of energy based on the movements of the human body in daily life, such as arm waving, walking, running, and arm and knee bending.[12–15] Previous studies have indicated that T-TENGs can be coated with polyvinylidene fluoride (PVDF), PTFE, and polydimethylsiloxane (PDMS) to increase the frictional surface area.[16–26] Moreover, a high electrical output has been achieved using metals with hard properties as friction materials, for example, Au, Ag, and Cu. However, previous studies did not consider the durability against complex manufacturing processes and twisting or bending deformation compared with the output power. In particular, the T-TENGs generated high energy only in the intentional vertical contact mode. The generated power was high when the area was large; however, the lifespan was short.[27] Therefore, it is necessary to develop a T-TENG that can efficiently harvest energy in various modes, including the vertical-contact mode, and that does not deteriorate in terms of durability under the effects of shape deformation and external forces.

Somkuwar's work[28] proposed a breathable-fabric-based TENG with an open-porosity polydimethylsiloxane coating. To enhance the triboelectric performance and wearable comfort, sacrificial templates, including insoluble NaCl, DBP, and soluble silicone oil, were applied to synergistically construct open porous structures. The open porous structure not only benefits the air permeability but also enhances the triboelectric output owing to the increased contact area through an application experiment.

Chung's study[29] proposed a stretchable FTENG using polydimethylsiloxane and 2D-polyester fibers to improve the energy-harvesting performance. An MN-FTENG with a microneedle structure was fabricated using polymethyl methacrylate (PMMA) to develop a wearable device with high elasticity and conductivity. Experiments demonstrated that FTENGs with microstructures had approximately 34–37% higher output voltage and current than FTENGs without microstructures, and that motion detection could be performed based on the movements of large joints such as elbows and knees.

Song's study[30] proposed a flexible large-scale fiber-based TENG using a knitted Chinese fabric coated with silver and a PDMS film. To improve the electrical performance, the proposed TENG inserted a pattern on the surface of the PDMS film using rough sandpaper from the microstructured arrays.

Through experiments, it was verified that as the degree of surface coating of the sandpaper increased, the effective contact surface expanded to improve the electrical performance, and excessive fine pores could degrade the electrical performance.

In this paper, we propose a flexible sandwich-structured T-TENG (STENG) that can harvest energy based on the motion of the human body by effectively using textile strength. To solve the problems associated with previous T-TENGs, one side of the STENG was coated with a micropatterned EcoFlex. Moreover, to generate output power during various operations, the stretchability was improved by attaching the acetate cloth of the winding structure to the textile side of the STENG. Based on the friction generated between the micropatterned EcoFlex coating and acetate, the STENG could harvest mechanical energy in the vertical contact, stretching, and rubbing modes. The STENG generates a maximum voltage of 361.4 V and power of 58.2 μA in the vertical contact mode, resulting in a 250% increase in the output performance compared to the non-patterned planar-EcoFlex-based STENG. Moreover, 135 light-emitting diodes (LEDs) are successfully operated using the output power of the STENG without an external power source, demonstrating excellent durability and potential applicability. The proposed STENG is a self-powered device that can supply power to small portable electronic devices and is expected to be widely used in energy-harvesting systems in the future.

Experimental details

As shown in Fig. 1a, the STENG has a sandwich-type structure made of two stretchable textiles and is manufactured using four materials with excellent flexibility and elasticity. Fig. 1b shows the STENG fabrication process. One stretchable textile is coated with micropatterned EcoFlex (charge affinity, -72 nC J^{-1}) and used as a negative friction material. Power generation performance was improved by patterning the EcoFlex surface based on the microstructure of crepe paper.[31–34] The nanostructured surface of the microstructure-based EcoFlex is clearly visible in the SEM images. Copper wires were used as electrodes in all the triboelectric layers. The stretchable textile on the other side was used as the positive friction material by attaching an acetate cloth to the winding structure. Because this is a serpentine structure, it can be expanded and contracted up to 50% in the lateral direction. The lower textile can be stretched by up to 13% owing to the acetate cloth of the winding structure attached to the surface. The top surface of the acetate cloth was sewn with yarn to create an air gap, which could generate energy even in the stretching mode. In other words, based on the friction generated between the micropatterned EcoFlex surface and acetate, the STENG can harvest mechanical energy in the contact–separate, stretching, and rubbing modes. In addition, because flexible materials were used, the structure was free from deformations. The total area of the fabricated STENG is 5 × 8 cm^2, and the thickness is 40 ± 5 mm. As STENG use flexible and elastic materials, they can generate electrical outputs in various modes.

Fig. 2 shows the working principle of the STENG operating in the contact–separation mode. In the STENG, the friction
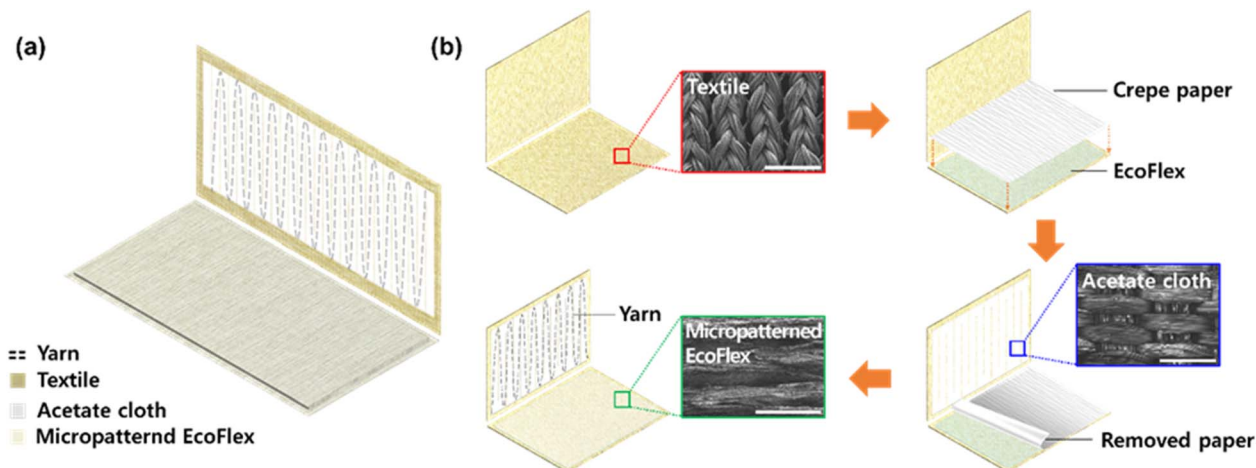
Fig. 1 (a) Stretchable TENG with a surface area of 5 × 8 cm². (b) STENG fabrication process. The inset shows a scanning electron microscope (SEM) image of the textile and acetate cloth with a scale bar of 500 nm. The coated micropatterned EcoFlex surface at a scale bar of 1000 mm.

between the acetate cloth and the micropatterned EcoFlex coating causes electrons to move in the electrode and generate a current. As shown in Fig. 2a, the STENG initially possessed no charge on its contact surfaces and electrodes. When an external force was applied to the STENG, the upper acetate cloth and the less micropatterned EcoFlex came into contact. At this point, the upper and lower textiles are negatively and positively charged, respectively. As shown in Fig. 2b, when the two triboelectric materials are separated and retain their original shapes, the opposite charges of each material are quickly separated by the voids. When the two materials are separated, a potential difference develops between the electrodes, and electrons flow from the top electrode to the bottom electrode until the charge accumulates. As shown in Fig. 2c, when the two materials were separated as much as possible and reached equilibrium.

As shown in Fig. 3, the performance was evaluated by measuring and comparing the electrical outputs of the STENG (area of 5 × 8 cm²). A digital oscilloscope with an internal impedance of 1 MΩ and precision source/measurement device (B2911A) were used to measure the output power of the STENG. A STENG made of all-stretchable materials can perform repeated shape transformations, such as bending or stretching. In the STENG, the surface charge density increased because of the EcoFlex surface of the microstructure on the crepe paper. As shown in Fig. 3a and b, the voltage and current of the STENG were measured in the vertical contact–separation mode. When a force of ~1 kgf was applied, the output voltage and current of the patterned STENG were determined to be 361.4 V and 58.2 µA, respectively. The STENG with the winding structure of the acetate cloth stretched up to 50% in the transverse direction.
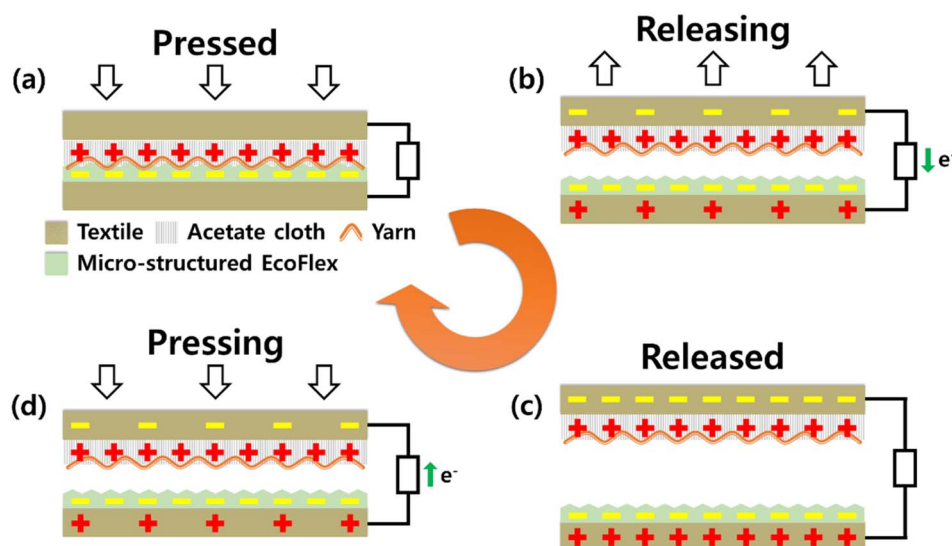

Fig. 2 STENG mechanism. (a) External force applied to the STENG and compressed. (b) Triboelectric layer of STENG separated. (c) Triboelectric layer of the STENG is completely separated. (d) When an external force was applied again, STENG was compressed.
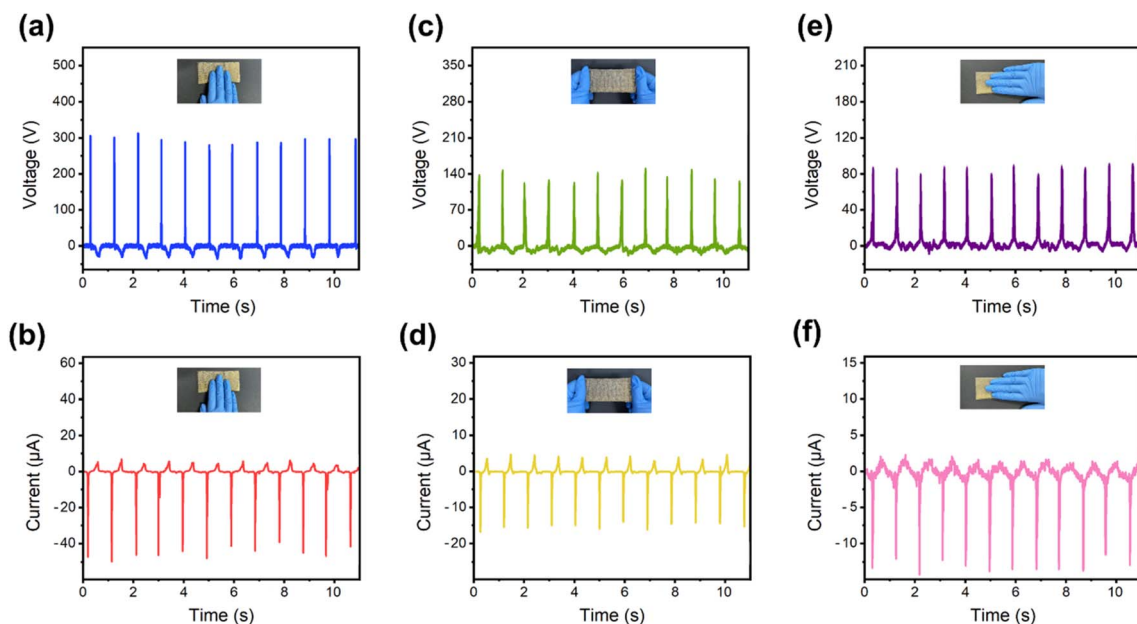
Fig. 3 Comparison of the electrical output power and current performance of the three types of the STENG; (a and b) contact–separation (361.4 V and 58.2 μA), (c and d) stretchable (214.7 V and 25 μA), and (e and f) rubbing (166.2 V and 23 μA) modes.

Therefore, as shown in Fig. 3(c and d), the STENG-measured voltage and current in the stretching mode were 166.2 V and 23 μA, respectively. The STENG can measure the voltage and current in the rubbing mode based on the characteristics of the four materials used. As shown in Fig. 3(e and f), the STENG generated a maximum output of 119.5 V and 17 μA considering the patterned surface according to the repeated rubbing operation. This led to a 250% increase in the output performance compared to the planar-EcoFlex-based STENG without micropatterns. The STENG can obtain output power in the vertical contact, stretching, and rubbing modes because flexible materials such as textiles are used.

Results and discussion

To prove the optimal output performance of the STENG, various patterns were coated on the surface of EcoFlex, and the outputs were compared. Fig. 4(a–d) show the SEM images of the EcoFlex non-patterned coating, microstructure of the crepe paper, air form, and Teflon cloth pattern. The SEM analysis of the fabricated pattern-based EcoFlex was conducted at 100 μm and 500 μm scale bars, showing the array of patterns, surface texture, and microstructure of the surface. Fig. 4a shows the surface of a textile coated with EcoFlex without a specific pattern. Fig. 4b shows a surface image of the textile coated with EcoFlex in an air-form pattern, and it was confirmed that the surface was irregular and uneven. A STENG using an air-foam-based EcoFlex has fine holes formed by air foam; thus, the air permeability and flexibility are improved. Fig. 4c shows the surface image of a textile coated with EcoFlex and a Teflon cloth pattern with a high negative charge affinity, showing a regular and even array. Fig. 4d shows the surface of a textile coated with microstructured EcoFlex using the microstructure of the crepe paper. The output voltage and current

of the STENG were measured in the contact–separation mode by deploying four coating patterns on the surface of the EcoFlex. As shown in Fig. 4(e and f), a relatively low voltage of 155.9 V and current of 11 μA were evident when EcoFlex without a pattern was used as the negative triboelectric layer. The STENG using an air-foam-based EcoFlex improved the air permeability and flexibility owing to air-foam formation; however, noise was severe owing to excessive micropores and irregular patterns, and the output voltage and current were relatively low. This structure shows a maximum voltage of 172.3 V and an unstable current of 19 μA. In the case of Teflon cloth pattern-based EcoFlex, a stable power with a voltage of 215.7 V and current of 28 μA was determined; however, the output performance was lower than that of the crepe-paper-microstructure-based STENG. Through electrical characterization experiments, it was demonstrated that EcoFlex, based on the microstructure of crepe paper, has a sophisticated geometric structure and regular arrangement, which can improve the frictional area and electrical output and increase the efficiency of the STENG power generation process.

Fig. 5 shows the mechanical and electrical characteristics of the STENG. As shown in Fig. 5a, the tensile strength was measured using a tensile tester (MCT-2150) to evaluate the mechanical properties of the STENG. Tensile tests can be used to measure the maximum stress until the material is segregated by the tensile load generated when it is stretched from both sides. A constant-speed tensile tester was used to obtain the force–strain diagram. As shown in Fig. 5b, the STENG increased the strain at a constant rate and generated a maximum load of 5.8 N. It was not damaged even at a high strain rate because of its highly flexible materials, such as acetate cloth and micro-patterned EcoFelx, for the winding structure. The power density was measured by connecting a load resistance of $10–10^{15}$ Ω to the STENG electrode. As shown in Fig. 5c, when the load
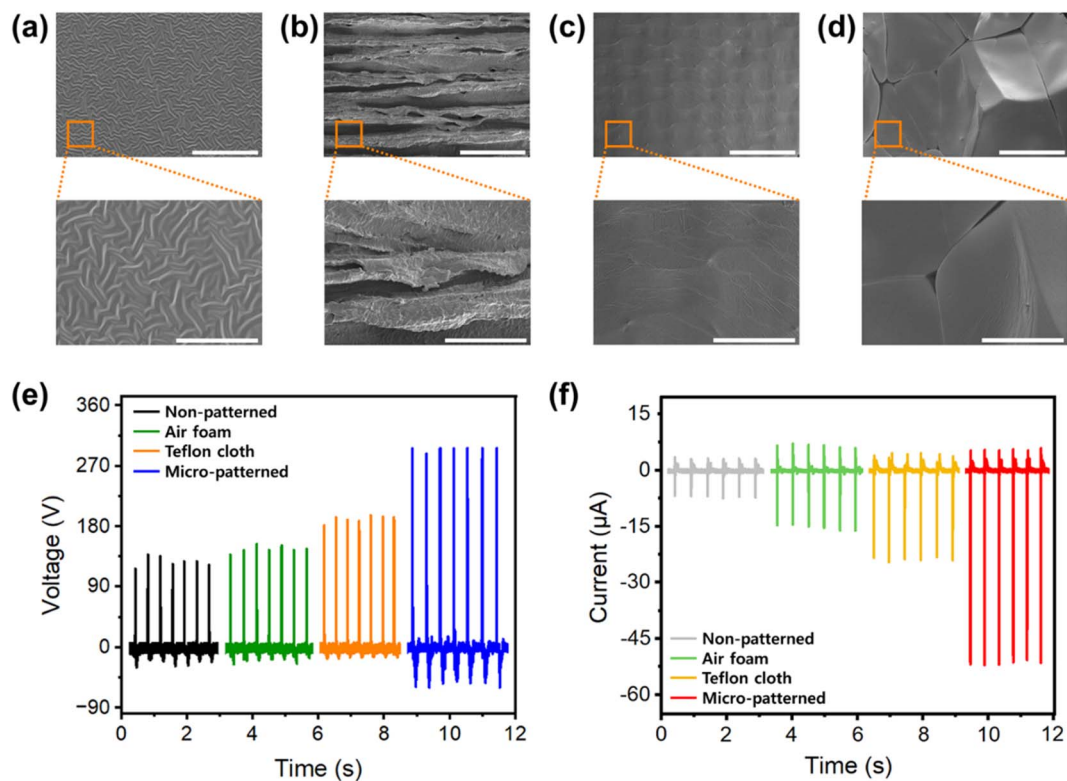
Fig. 4 Microstructured EcoFlex-based STENG with a high electrical output. (a–d) SEM images of non-patterned, air foam, Teflon cloth, and crepe paper show a scale bar of 1 μm. (e and f) Comparison between the output voltage and current under different EcoFlex patterns.
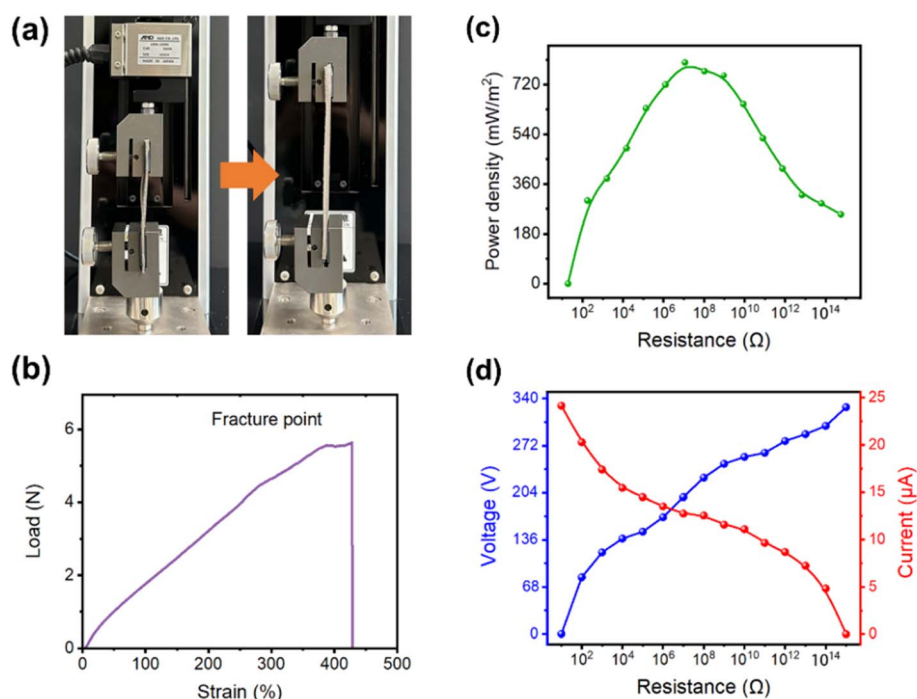

Fig. 5 (a) Experimental setup for the tensile strength test. (b) Load–deformation curve. (c) Output voltage and current based on the external load resistance. (d) Power density across various loading resistors.

resistance increased, the output voltage increased and then saturated; however, the output current decreased according to Ohm's law. The output power density is calculated as $P = I^2R$. The maximum output power density is obtained when the load resistance is equal to the internal impedance of the STENG. As shown in Fig. 4d, a maximum power density of 792 mW m^{-2} was obtained at a load resistance of 10^7 Ω.

To demonstrate the excellent mechanical durability of the STENG, the output voltage and current based on repetitive contact–separation motions were measured using a pushing tester. Using a pushing tester (JIPT-100), a constant pressure of 0.1 kgf was applied to the STENG in the vertical-contact separation mode. The pushing tester repeatedly applied pressure to the 1×1 cm area of the experimental sample at regular intervals and tested the durability by calculating the average value of the generated voltage and current. As shown in Fig. 6a, when a force of ~0.1 kgf for 5000 cycles was applied, the output voltage exhibited an error range of up to 0.4 V. As shown in Fig. 6b, in the same experimental environment, the output current exhibited a low error range of up to 0.6 μA. To prove the
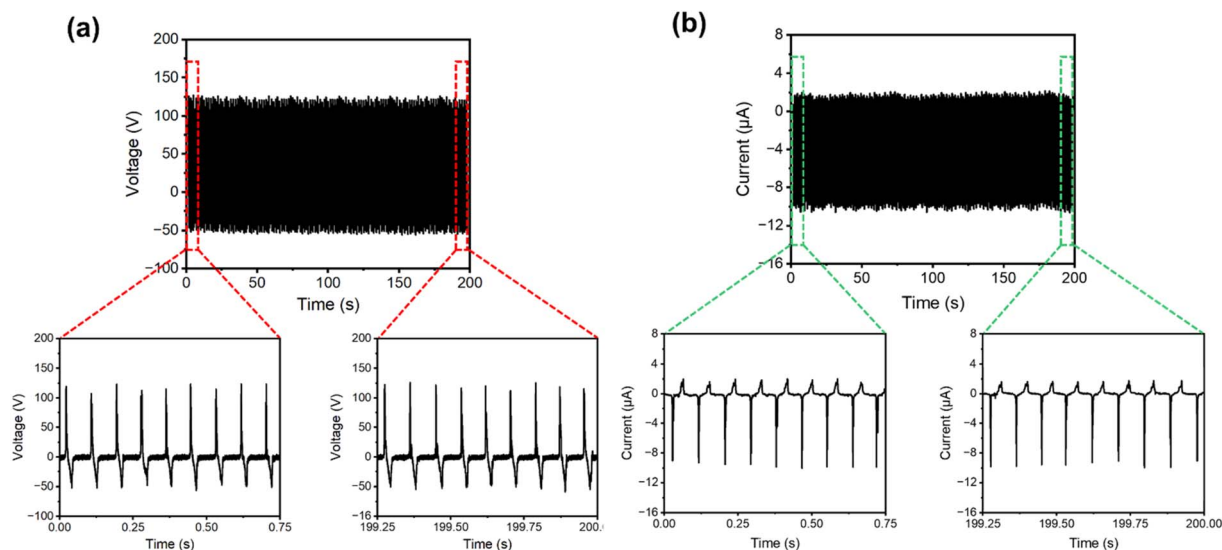

Fig. 6 Mechanical durability test of the STENG. (a) Output voltages of the cycled compressive force on the STENG over 5000 cycles. The voltage output in the initial phase and after 5000 cycles. (b) Current of the cycled compressive force on the STENG over 5000 cycles. Current in the initial phase and after 5000 cycles.
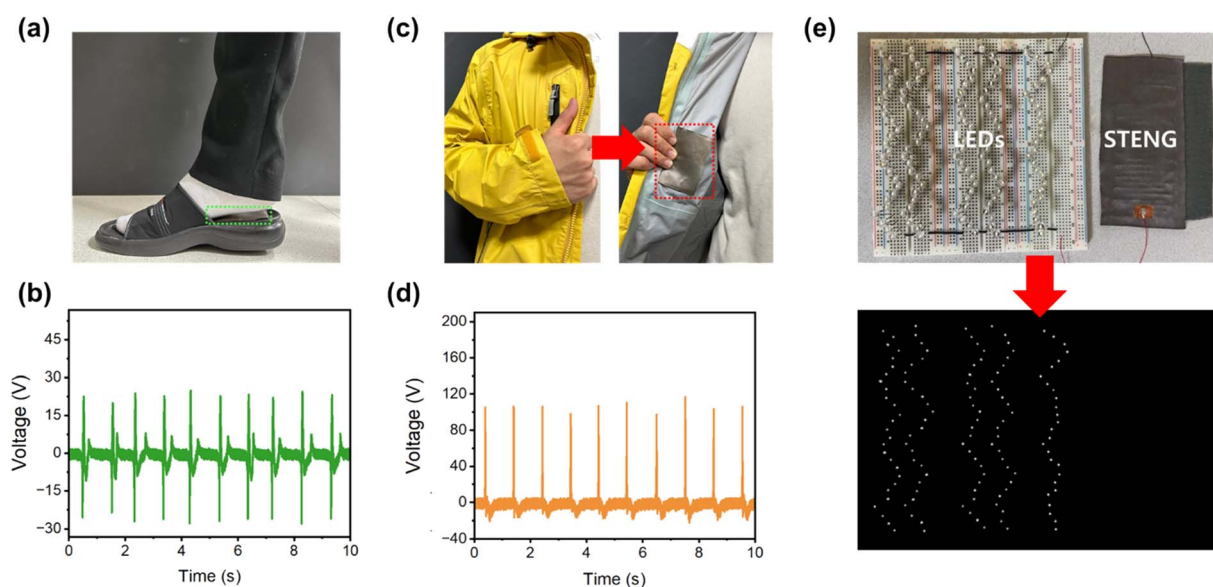

Fig. 7 STENG harvesting energy from human motion. (a) STENG attached to the shoe sole. (b) Output voltage generated by the STENG mounted on the shoe. (c) STENG integrated with a coat harvesting energy from the movement of clothes. (d) Output voltage generated by the STENG attached to the cloth. (e) STENG can be used to continuously illuminate several LEDs *via* tapping.

durability of the STENG in the stretching and rubbing modes, the voltage and current were measured through repetitive motion for 60 s. As shown in Fig. 6, the output voltage and current of the STENG in the stretching mode showed an error range of up to 20 V and 2.4 μA. Moreover, in the rubbing mode, the STENG showed a maximum voltage of 12 V and an error range of 3.2 μA current. The error was calculated by comparing the initial and later outputs. Therefore, the STENG exhibited excellent mechanical durability and stability as it produced a constant signal without a significant decrease in the electrical output, and its electrical output performance did not deteriorate even after repeated deformation for 5000 cycles.

To demonstrate the potential of the STENG, the output voltage generated by the motion of a human was measured. As shown in Fig. 7(a–d), the STENG can obtain power in daily life by attaching it to a commercial coat or shoe sole.[35] Fig. 7a shows a STENG attached to the shoe sole. When a human walks, a constant voltage of ~50 V is generated by the contact between the STENG and the heel (Fig. 7b). As shown in Fig. 7c, the STENG attached to the coat harvests energy based on the movement of the cloth. Fig. 7d shows the output generated by the STENG when the coat was moved, which resulted in an average voltage of 112 V. These experimental results demonstrate that the STENG can harvest biomechanical energy from various types of body movements. As shown in Fig. 7e, using the STENG, it was possible to turn on LEDs connected in series based on the power generated from the motion. Thus, STENG with excellent flexibility, durability, and stability can be used in portable and wearable power systems.

Conclusions

We fabricated a stretchable and fully flexible STENG for use in wearable energy-harvesting devices. Based on the friction generated between the micropatterned EcoFlex and acetate, the STENG harvested mechanical energy in the vertical contact, stretching, and rubbing modes. The output voltages and currents of 361.4 V and 58.2 μA in the contact–separate mode, 166.2 V and 23 μA in the stretching mode, and 119.5 V and 17 μA in the rubbing mode were obtained. This resulted in a 250% improvement in the output performance compared with the flat EcoFlex-based STENG without micropatterns. In addition, excellent durability was demonstrated without a drop in the output power during repetitive pushing motions for 5000 cycles. The STENG operated up to 135 LEDs using its output power in the vertical contact, stretching, and rubbing modes. These findings can provide a textile-based power source for practical applications in e-textiles and self-powered electronics in the future.

Conflicts of interest

The authors declare no competing financial interest.

Acknowledgements

References

1 N. Niknejad, W. B. Ismail, A. Mardani, H. Liao and I. Ghani, A comprehensive overview of smart wearables the state of the art literature, recent advances, and future challenges, *Artif. Intell.*, 2020, **90**, e103529.

2 Z. Wu, T. Cheng and Z. L. Wang, Self-powered Sensors and Systems Based on Nanogenerators, *Sensor*, 2020, **20**, 2925.

3 K. R. S. D. Gunawardhana, N. D. Wanasekara and R. D. I. G. Dharmasena, Towards Truly Wearable Systems Optimizing and Scaling Up Wearable Triboelectric Nanogenerators, *iScience*, 2020, **23**, e101360.

4 K. Dong and Z. L. Wang, Self-charging power textiles integrating energy harvesting triboelectric nanogenerators, *J. Semicond.*, 2021, **42**, e101601.

5 D. W. Kim, J. H. Lee, J. K. Kim and U. Jeong, Material aspects of triboelectric energy generation and sensors, *NPG Asia Mater.*, 2020, **12**, 1–17.

6 F. R. Fana, Z. Q. Tian and Z. L. Wang, Flexible triboelectric generator, *Nano Energy*, 2012, **1**, 328–334.

7 R. Hinchet, W. Seung and S. W. Kim, Recent Progress on Flexible Triboelectric Nanogenerators for Self Powered Electronics, *ChemSusChem*, 2015, **8**, 2327–2344.

8 W. Paosangthonga, M. Wagiha, R. Toraha and S. Beeby, Textile-based triboelectric nanogenerator with alternating positive and negative freestanding grating structure, *Nano Energy*, 2019, **66**, e104148.

9 Y. Hua and Z. Zheng, Progress in textile-based triboelectric nanogenerators for smart fabrics, *Nano Energy*, 2019, **56**, 16–24.

10 W. Paosangthong, R. Torah and S. Beeby, Recent progress on textile-based triboelectric nanogenerators, *Nano Energy*, 2019, **55**, 401–423.

11 K. Dong, X. Peng, R. Cheng and Z. L. Wang, Smart Textile Triboelectric Nanogenerators Prospective Strategies for Improving Electricity Output Performance, *Nanoenergy Advances*, 2022, **2**, 133–164.

12 J. Liu, L. Gu, N. Cui, Q. Xu, Y. Qin and R. Yang, Fabric-Based Triboelectric Nanogenerators, *SPJ*, 2019, **2019**, e1091632.

13 P. Huang, D. L. Wen, Y. Qiu, M. H. Yang, C. Tu, H. S. Zhong and X. S. Zhang, Textile-Based Triboelectric Nanogenerators for Wearable Self-Powered Microsystems, *Micromachines*, 2021, **12**, 158.

14 S. S. Kwak, H. J. Yoon and S. W. Kim, Textile-Based Triboelectric Nanogenerators for Self-Powered Wearable Electronics, *Adv. Funct. Mater.*, 2018, **29**, e1804533.

15 C. Fan, Y. Zhang, S. Liao, M. Zhao, P. Lv and Q. Wei, Manufacturing Technics for FabricFiber-Based Triboelectric Nanogenerators, *Nanomaterials*, 2022, **12**, 2703.

16 Y. T. Jaoa, P. K. Yanga, C. M. Chiua, Y. J. Lina, S. W. Chena, D. Choid and Z. H. Lin, A textile-based triboelectric

nanogenerator with humidity-resistant output, *Nano Energy*, 2018, **50**, 513–520.

17 A. Y. Choi, C. J. Lee, J. Park, D. Kim and Y. T. Kim, Corrugated Textile based Triboelectric Generator for Wearable Energy Harvesting, *Sci. Rep.*, 2017, **7**, 45583.

18 C. C. Chang, J. F. Shih, Y. C. Chiou, R. T. Lee, S. F. Tseng and C. R. Yang, Development of textile-based triboelectric nanogenerators integrated with plastic metal electrodes, *Int. J. Adv. Des. Manuf. Technol.*, 2019, **104**, 2633–2644.

19 I. Aazem, D. T. Mathew, S. Radhakrishnan, K. V. Vijoy, H. John, D. M. Mulvihill and S. C. Pillai, Electrode materials for stretchable triboelectric nanogenerator in wearable electronics, *RSC Adv.*, 2022, **12**, 10545.

20 L. Liu, X. Yang, L. Zhao, W. Xu, J. Wang, Q. Yang and Q. Tang, Nanowrinkle-patterned flexible woven triboelectric nanogenerator toward self-powered wearable electronics, *Nano Energy*, 2020, **73**, 104797.

21 D. L. Wena, X. Liua, H. T. Denga, D. H. Suna, H. Y. Qiana, J. Brugger and X.-S. Zhang, Printed silk-fibroin-based triboelectric nanogenerators for multi-functional wearable sensing, *Nano Energy*, 2019, **66**, 104123.

22 M. Zhu, Q. Shi, T. He, Z. Yi, Y. Ma, B. Yang, T. Chen and C. Lee, Self-Powered and Self-Functional Cotton Sock Using Piezoelectric and Triboelectric, *ACS Nano*, 2019, **13**, 1940–1952.

23 T. He, H. Wang, J. Wang, X. Tian, F. Wen, Q. Shi, J. S. Ho and C. Lee, Self-Sustainable Wearable Textile Nano-Energy Nano-System (NENS) for Next-Generation Healthcare Applications, *Adv. Sci.*, 2019, **6**, 1901437.

24 J. Xiong, P. Cui, X. Chen, J. Wang, K. Parida, M. F. Lin and P. S. Lee, Skin-touch-actuated textile-based triboelectric nanogenerator with black phosphorus, *Nat. Commun.*, 2018, **9**, 4280.

25 Z. B. Li, H. Y. Li, Y. J. Fan, L. Liu, Y. H. Chen, C. Zhang and G. Zhu, Small-Sized, Lightweight, and Flexible Triboelectric Nanogenerator, *ACS Appl. Mater. Interfaces*, 2019, **11**, 20370–20377.

26 M. S. Medeiros, D. Chanci, C. Moreno, D. Goswami and R. V. Martinez, Waterproof, Breathable, and Antibacterial Self-Powered e-Textiles Based on Omniphobic Triboelectric Nanogenerators, *Adv. Funct. Mater.*, 2019, **29**, 1904350.

27 Z. Lin, J. Yang, X. Li, Y. Wu, W. Wei, J. Liu, J. Chen and J. Yang, Large-Scale and Washable Smart Textiles Based on Triboelectric Nanogenerator Arrays for Self-Powered Sleeping Monitoring, *Adv. Funct. Mater.*, 2017, **28**, 1704112.

28 V. U. Somkuwar, A. Pragya and B. Kumar, Influence of the Fabric Topology on the Performance of a Textile-Based Triboelectric Nanogenerator for Self-Powered Monitoring, *J. Mater. Sci.*, 2020, **55**, 5177–5189.

29 C. Chung, Y. Huang, T. Wang and Y. Lo, Fiber-Based Triboelectric Nanogenerator for Mechanical Energy Harvesting and Its Application to a Human–Machine Interface, *Sensors*, 2022, **22**, 9632.

30 J. Song, L. Gao, X. Tao and L. Li, Ultra-Flexible and Large-Area Textile-Based Triboelectric Nanogenerators with a Sandpaper-Induced Surface Microstructure, *Materials*, 2018, **11**, 2120.

31 Y. Zhou, W. Deng, J. Xu and J. Chen, Engineering Materials at the Nanoscale for Triboelectric Nanogenerators, *Cell Rep. Phys. Sci.*, 2020, **1**, 100142.

32 X. S. Zhang, M. D. Han, R. X. Wang, B. Meng, F. Y. Zhu, X. M. Sun, W. Hu, W. Wang, Z. H. Li and H. X. Zhang, High-performance triboelectric nanogenerator with enhanced energy density based on single-step fluorocarbon plasma treatment, *Nano Energy*, 2014, **4**, 123–131.

33 W. Seung, M. K. Gupta, K. Y. Lee, K. S. Shin, J. H. Lee, T. Y. Kim, S. Kim, J. Lin, J. H. Kim and S. W. Kim, Nanopatterned Textile-Based Wearable Triboelectric Nanogenerator, *ACS Nano*, 2015, **9**, 3501–3509.

34 W. Zhong, B. Xu and Y. Gao, Engraved pattern spacer triboelectric nanogenerators for mechanical energy harvesting, *Nano Energy*, 2022, **92**, 106782.

35 T. Zhou, C. Zhang, C. B. Han, F. R. Fan, W. Tang and Z. L. Wang, Woven Structured Triboelectric Nanogenerator for Wearable Devices, *ACS Appl. Mater. Interfaces*, 2014, **6**, 14695–14701.